

ORIGINAL ARTICLE

Open Access

# Preparation of nanostructured TiO<sub>2</sub>-based photocatalyst by controlling the calcining temperature and pH

Mohammed Jasim Uddin, Md Akhtarul Islam, Sheikh Ariful Haque, Saidul Hasan, Mohammad Shaiful Alam Amin\* and Mohammed Mastabur Rahman

## Abstract

Nanostructured TiO<sub>2</sub> has been synthesized using one-step sol-gel method and characterized by different characterization techniques (SEM, EDS, XRD, and UV-vis spectroscopy). The photocatalytic degradation of methylene blue (MB) and Congo red (CR) is studied with the synthesized TiO<sub>2</sub>. The photocatalytic degradation data has been validated using several kinetic models. The TiO<sub>2</sub> showed efficient photocatalytic degradation performance on MB and CR. In addition to this, the effect of pH on the photocatalytic degradation has been investigated. The TiO<sub>2</sub> showed enhanced photocatalytic performance in basic media than that in neutral or acidic ones.

**Keywords:** Photocatalyst, Titanium dioxide, Sol-gel method, Photocatalytic degradation kinetics

## Background

Titanium dioxide is a promising material and is widely used in many applications such as disinfection, medical treatment, environmental purification, and photovoltaic cell [1,2] due to its high photocatalytic activity [3,4], excellent gas-sensitivity [5], and dielectric properties [6]. TiO<sub>2</sub> particles, which are smaller than tens of nanometers, are of particular interest for the synthesis of new materials due to their special optical properties, high catalytic activity, and unusual mechanical properties in comparison to their bulk material counterpart [7]. TiO<sub>2</sub> can be synthesized into various shapes - nanoporous materials, nanoparticles, nanowires, nanorods, nanotubes, and nanofibers using different preparation methods [5]. Many methods have been developed to control the size of nanoparticles, which include Langmuir-Blodgett films [8], vesicles [9], and reverse micro-emulsion method [10]. The chemical and physical properties exhibited by these materials depend on both the composition and the degree of homogeneity. Therefore, different synthesis strategies have been developed. These studies include coprecipitation, flame hydrolysis, impregnation, and chemical vapor deposition [11,12]. So far, sol-gel route has

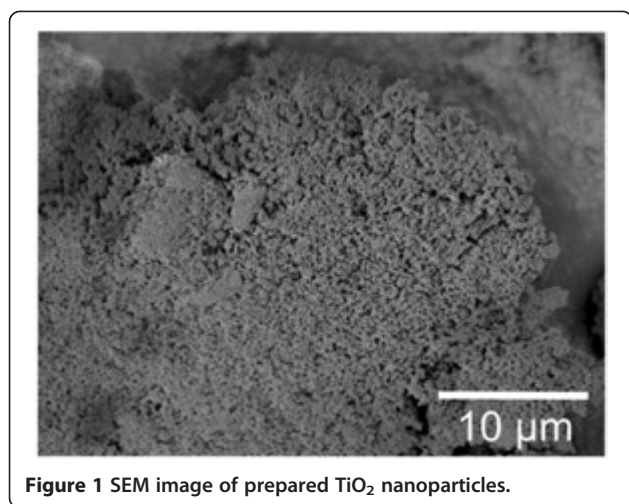
demonstrated a high potential for controlling the bulk and surface properties of the oxides [13-15]. Additionally, non-hydrolytic sol-gel routes have been reported in the literature [16]. The physical and chemical properties of TiO<sub>2</sub> in the nanometer size range depend on phase composition, grain size, and dispersity [17]. Nanosized TiO<sub>2</sub> crystals, of less than 10 nm, show significant differences with the bulk TiO<sub>2</sub> in many aspects due to the quantum size effect [18,19].

The photocatalytic oxidation technology is frequently used for the complete degradation of organic micropollutants (dyes) in water, utilizing sunlight and UV radiation as energy sources [13,20]. However, TiO<sub>2</sub> is active only under near-ultraviolet irradiation region, because of its wide-bandgap energy of 3.0 to 3.2 eV. As a result, significant efforts have been made over the last two decades to develop modified TiO<sub>2</sub> particles that are functioning under visible-light irradiation ( $\lambda > 400$  nm). TiO<sub>2</sub> has been used in a wide range of application including thin films or as submicron powders [21].

In the present paper, 20 g of nanostructured TiO<sub>2</sub> powder is synthesized from Ti (O-iC<sub>3</sub>H<sub>7</sub>)<sub>4</sub> (referred to hereafter as TIP) without the addition of catalyst or stabilizer at room temperature and atmospheric pressure. Under such conditions, nanosized particles (20 to 60 nm) are partly crystallized in the anatase phase. The

\* Correspondence: saikat\_cep@yahoo.com

Department of Chemical Engineering and Polymer Science, Shahjalal University of Science and Technology, Sylhet 3114, Bangladesh



objective of this paper is threefold: (1) to investigate the photocatalytic activity of the synthesized TiO<sub>2</sub> on methylene blue (MB) and Congo red (CR), reactive dyes which are mostly used in textile processing industries, (2) to investigate and reveal the photocatalytic degradation kinetics using several mathematical models, and (3) to determine the pH level at which the photocatalytic reaction proceeds with acceptable reaction rate and completion of photocatalytic degradation.

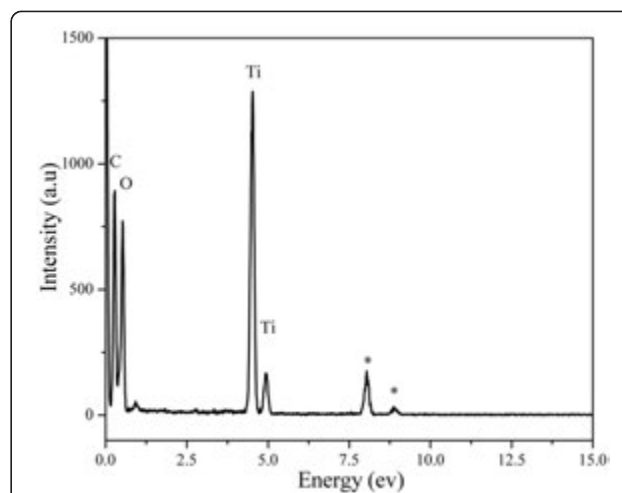
## Methods

### Materials

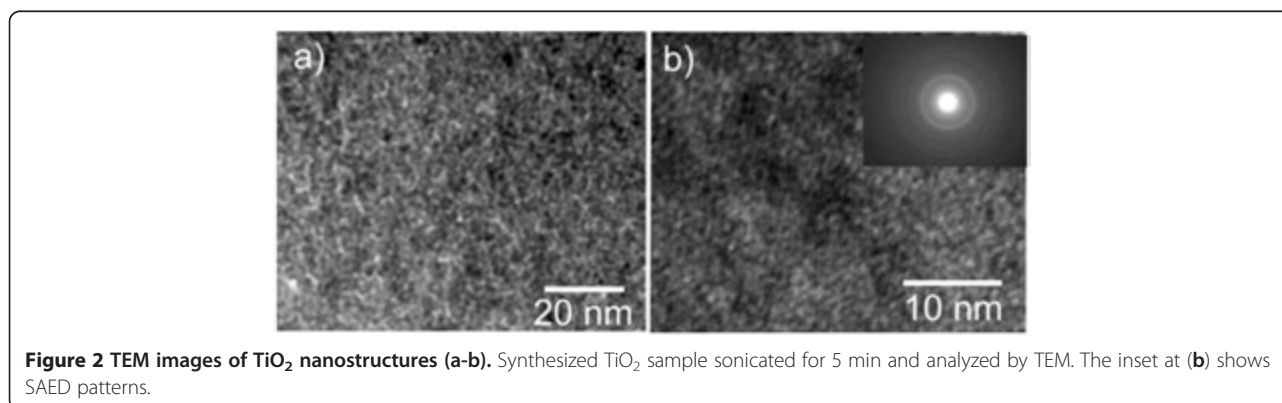
Titanium (IV) isopropoxide (Alfa Aesar, USA), 2-propanol (Alfa Aesar), MB (Merck, Germany), and CR (Merck) have been used as received. Water used in experiments was triple distilled and produced in laboratory. P25 (Degussa, Germany) was used as a reference photocatalyst (TiO<sub>2</sub>) throughout this study.

### Synthesis

Nanostructured TiO<sub>2</sub> was prepared by following sol-gel chemistry methods. The sol-gel method is a promising method, because the morphology of the nanomaterial is



varied simply by changing the solution composition and deposition condition. The synthesis reactor consists of a three-necked round bottom reactor equipped with a vertical condenser fitted to the middle neck. A separatory funnel was connected to one of the two side necks. Deionized water (24.13 mL) was added to 102.34 mL of 2-propanol under vigorous stirring to the remaining neck on the reactor. Following the addition of water, this neck was closed using a rubber stopper. Alkoxide precursor (50 mL) was added dropwise to the solution over a 4-h period using the separatory funnel fitted to the flask. This mixture was stirred continuously over a period of 24 h at room temperature. At this stage, a stable colloidal suspension of approximately 175 mL was formed. The excess water and alcohol were removed at room temperature and 10 kPa pressures using a rotary evaporator (Buchi R2015, BÜCHI Labortechnik AG, Switzerland) over a 7-day period. Approximately, 20 g of titania was obtained using this procedure.



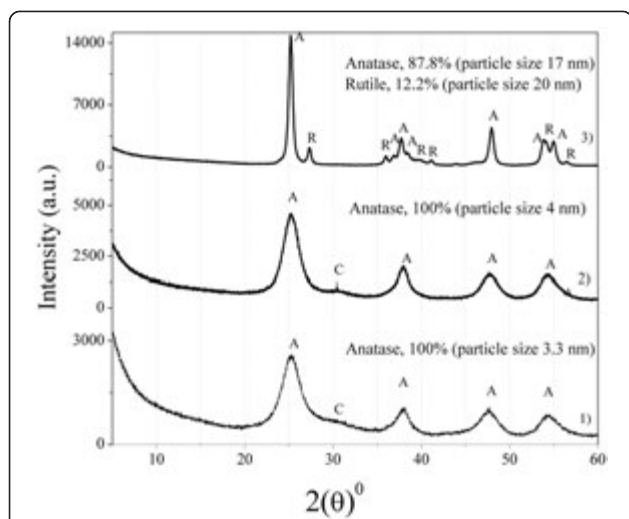


**Figure 4** XRD patterns of synthesized  $\text{TiO}_2$  calcined at different temperatures. Curve 1, 450°C; curve 2, 550°C; and curve 3, 650°C. A, anatase phase; R, rutile phase; C, carbon.

### Photocatalytic experiment

$\text{TiO}_2$  samples, each amounting 0.5 g, was taken into different ceramic crucibles and calcined in a muffle furnace

(JSMF-30 T, JS Research Inc., Korea) at 450°C, 550°C, and 650°C. The photocatalytic activity of titanium dioxides was studied by exposing the  $\text{TiO}_2$  samples, which contained MB and CR, to solar-like light. For photocatalytic reactions, the irradiation was carried out in solution at 308 K using a SOL 21500 lamp (SOL, Inc., USA). The SOL bulb yielded a spectrum very similar to natural sunlight ranging from ultraviolet to infrared radiation (approximately 295 to 3,000 nm). For this purpose, an aqueous solution (0.05% w/v) of reagent grade MB and CR was prepared for the impregnation of the reference and the synthesized  $\text{TiO}_2$  in the different volumetric flask. The same amount of each  $\text{TiO}_2$  sample was inserted under very mild stirring in the same amount of solution and remained there for 2 to 3 min to complete the mixing. The solution was then placed under the solar-like light (50 to 60 mW/cm<sup>2</sup>). UV-vis spectrum was recorded from the UV spectrophotometer (UV-1650, Shimadzu Corporation, Kyoto, Japan) in the wavelength range of 200 to 800 nm. The highest absorbance at 664 nm and 498 nm was recorded for MB and CR, respectively. The decrement of UV-vis band upon photocatalytic degradation was determined in an equal time interval. The pH (range 2 to 8) effect on photocatalytic

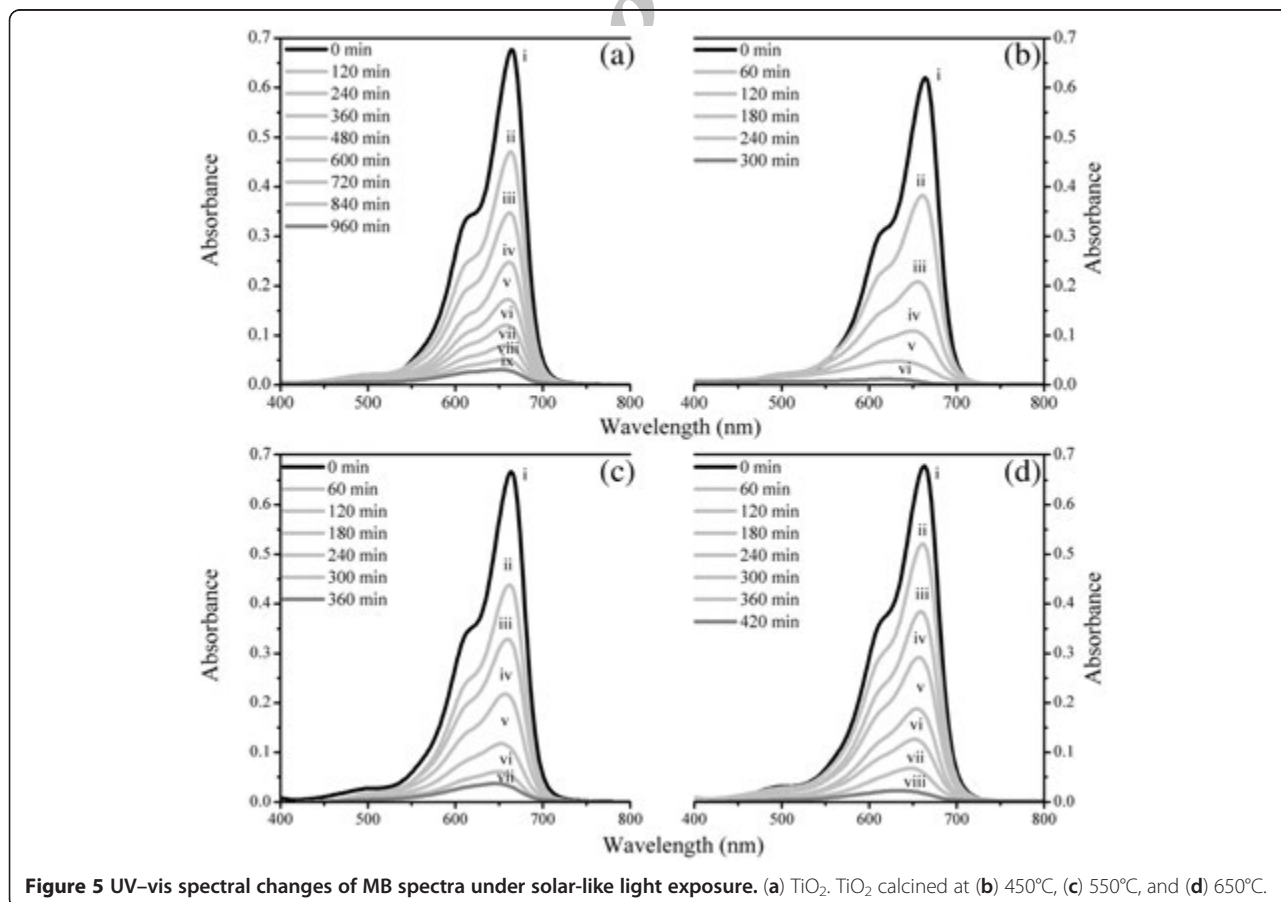


**Figure 5** UV-vis spectral changes of MB spectra under solar-like light exposure. (a)  $\text{TiO}_2$ .  $\text{TiO}_2$  calcined at (b) 450°C, (c) 550°C, and (d) 650°C.

degradation of MB and CR was investigated. The same experimental procedure was adopted for commercial P25 to compare with the synthesized one. The adsorption and photocatalytic degradation cycles were repeated twice on each sample to remove any experimental errors.

### Photocatalytic kinetic models

Four kinetic models were used to investigate the photocatalytic degradation profiles [22-24].

- (1) Zero-order model can be generally expressed as

$$C - C_0 = -kt \quad (1)$$

- (2) The first-order model expresses the photocatalytic degradation systems and can be generally written as

$$\log(C/C_0) = -kt \quad (2)$$

- (3) The parabolic diffusion model elucidates the diffusion-controlled photocatalytic degradation and the equation is as follows:

$$(1 - C/C_0)/t = kt^{-0.5} + a \quad (3)$$

- (4) The modified Freundlich model explains the experimental data on molecular ion exchange and

diffusion-controlled process with the following equation:

$$\log(1 - C/C_0) = \log k + b \log t \quad (4)$$

In these equations,  $C_0$  and  $C$  are the concentration of dyes at irradiation time 0 and  $t$ , respectively,  $k$  is the corresponding rate constant.

### Characterization techniques

Scanning electron micrographs (SEM) were obtained using a Hitachi-4800 field emission scanning microscope (Hitachi Ltd., Tokyo, Japan) operated at 3 kV to investigate the morphology. Transmission electron micrographs (TEM) were obtained using a JEOL 2010 (JEOL Ltd., Akishima, Tokyo, Japan) operated at 200 kV and equipped with an energy dispersive spectroscopic (EDS) microanalysis system (OXFORD Instruments, Oxfordshire, UK). The images were obtained using a CCD Mega Vision (III) camera (MegaVision, Inc., CA, USA).

The X-ray diffraction (XRD) patterns were obtained using a Bruker D5000 diffractometer (Bruker Daltonik GmbH, Bremen, Germany) equipped with a Cu-K $\alpha$  radiation of wavelength of 1.5418 Å. The accelerating voltage and the applied current were 45 kV and 40 mA, respectively.

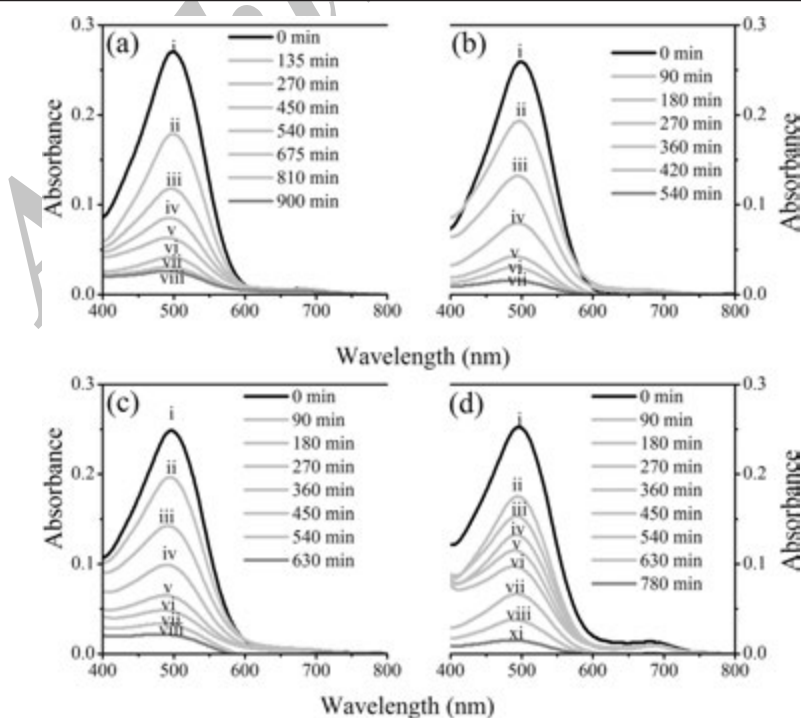


**Figure 6** UV-vis spectral changes of CR spectra under solar-like light exposure. (a)  $\text{TiO}_2$ .  $\text{TiO}_2$  calcined at (b) 450°C, (c) 550°C, and (d) 650°C.

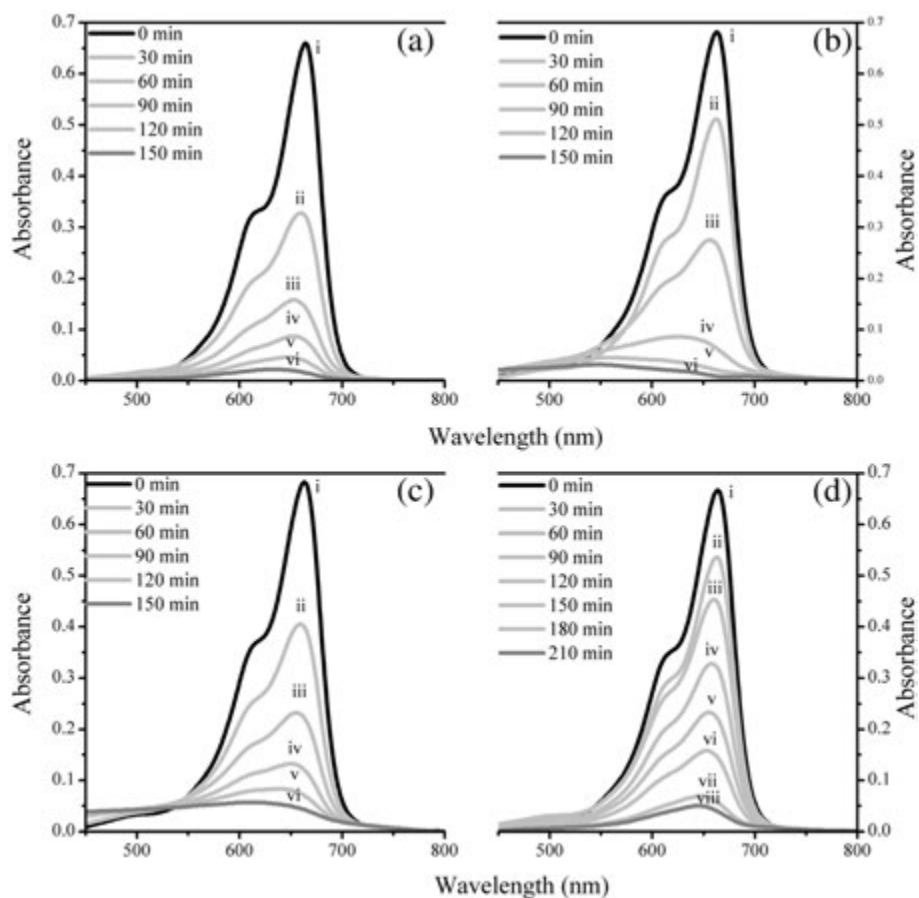


Figure 7 Spectral changes of MB spectra under solar-like light exposure. (a) P25. P25 calcined at (b) 450°C, (c) 550°C, and (d) 650°C.

## Results and discussion

### Morphology and structure analysis

The SEM image of the prepared TiO<sub>2</sub> nanoparticles by sol-gel method at room temperature (25°C) is shown in Figure 1. The TiO<sub>2</sub> aggregates consist of individual nanoparticles that are approximately in the range of 50 to 100 nm. The image shows that the supported

aggregates are lumped together with the large numbers of pores of very small dimensions. This feature suggests that the pores have a high surface area and can preferentially adsorb organic molecules or pollutants adhered to the surface. This feature suggests the uniformity of the aggregates. These particles consist of individual particles that are in the nanoscale range. A small portion of the

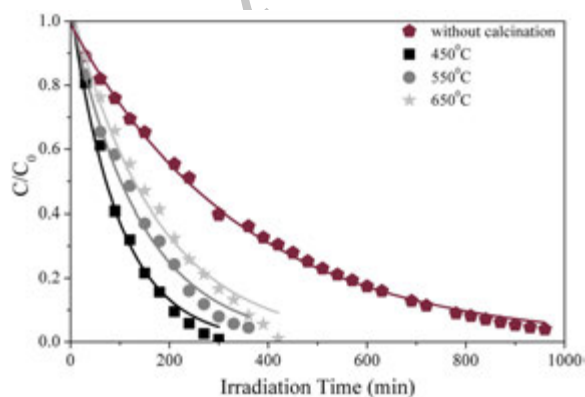


Figure 8 Photocatalytic degradation kinetics of MB on synthesized TiO<sub>2</sub>. Calcined at 450°C, 550°C, and 650°C.

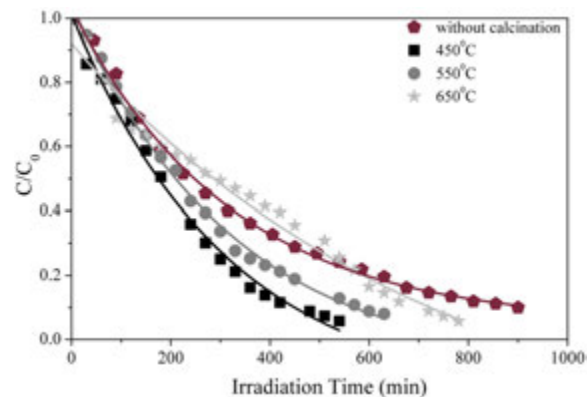
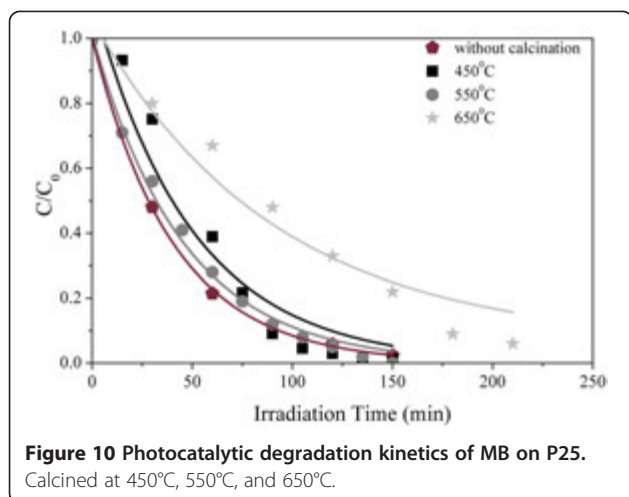


Figure 9 Photocatalytic degradation kinetics of CR on synthesized TiO<sub>2</sub>. Calcined at 450°C, 550°C, and 650°C.



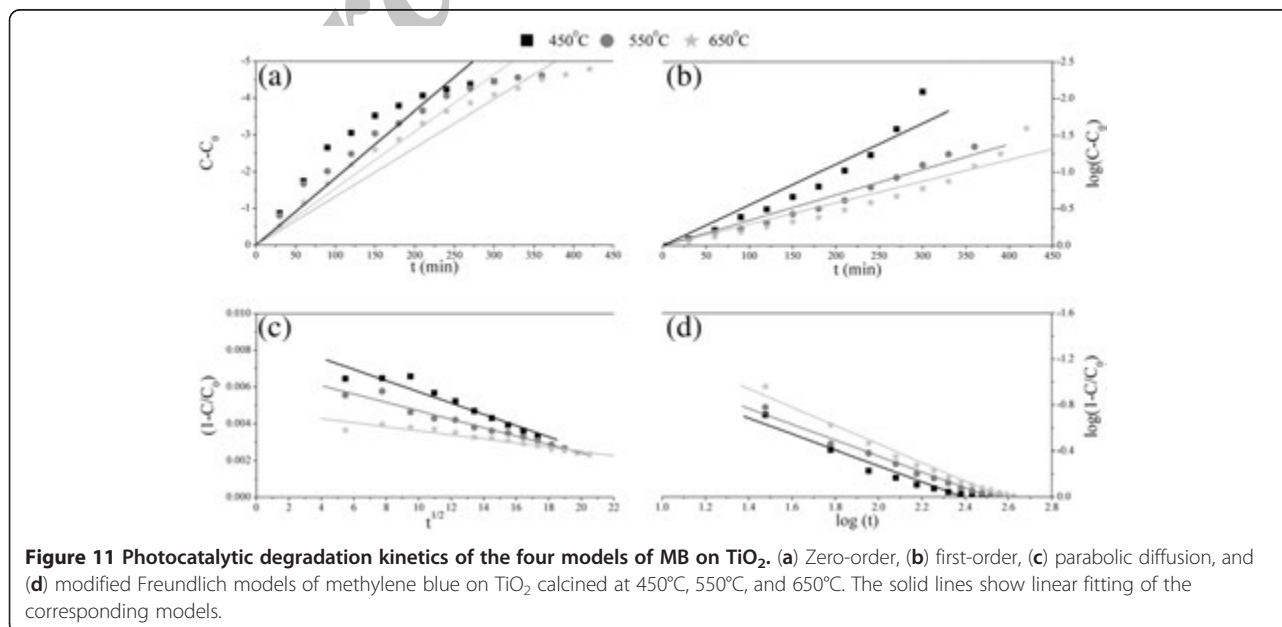
samples sonicated for 5 min and analyzed by TEM is shown in Figure 2. The structures of TiO<sub>2</sub> clusters consist of individual nanosized structures, which are approximately in the 50- to 60-nm range. The small size of TiO<sub>2</sub> nanoparticles suggests that the exposed surface area of the supported aggregates is very large, which is in agreement with the BET surface area analysis. The surface area and the average pore size ( $d_{BJH}$ ) of the synthesized nanostructure are found to be 545 m<sup>2</sup>g<sup>-1</sup> and 2.4 nm, respectively (BET plot and the pore size distributions are not shown for the sake of brevity). The nanostructured matrix is the origin of preferential adsorption of the organic molecule on the exposed surface which should undergo photocatalytic degradation by UV light illumination. EDS analysis, which is carried out during TEM analysis, shows only the titanium and

oxygen peaks (Figure 3). This implies that, following synthesis at low temperatures, the nanostructured support material is free of contaminants.

The XRD patterns of the synthesized TiO<sub>2</sub> calcined at different temperatures are reported in Figure 4 (curves 1 to 3). Curves 1 and 2 show three broad peaks and one intense peak at 38.0°, 47.5°, 54.20°, and 25.1°, respectively, which constitute the XRD pattern of TiO<sub>2</sub> of anatase phase. No additional peaks belonging to other phases are observed. The remarkable width of the peaks associated with the TiO<sub>2</sub> phase suggests that the size of the particle is quite small. From full width at half maximum (FWHM) of the peaks at 25.1° and 38.01°, as well as the use of Scherrer's equation,  $L_c = K\lambda/(\beta \cos\theta)$  [25] (where  $K$  is the shape factor, which has been assumed to be 0.9;  $\lambda$  is the x-ray wavelength;  $\beta$  is the FWHM of the diffraction line, and  $\theta$  is the Bragg's angle), an average particle diameter (3 to approximately 20 nm) can be calculated. This result is strongly consistent with the SEM and TEM results described above. In conclusion, by comparing the results from different techniques, the most efficient sample shows average particle diameter of 4 nm (Figure 4, curve 2). In fact, curve 3 shows a certain amount (12.2%) of rutile phase with comparatively larger particle size (17 to approximately 20 nm) due to calcination of the sample at the highest temperature (650°C).

#### Photocatalytic activity

The photocatalytic activity of TiO<sub>2</sub> has been investigated at high temperatures by exposing the reactor with MB and CR to UV light. In the absence of UV light irradiation, a reportable adsorption of dye molecules on the external TiO<sub>2</sub> surface causes the successive



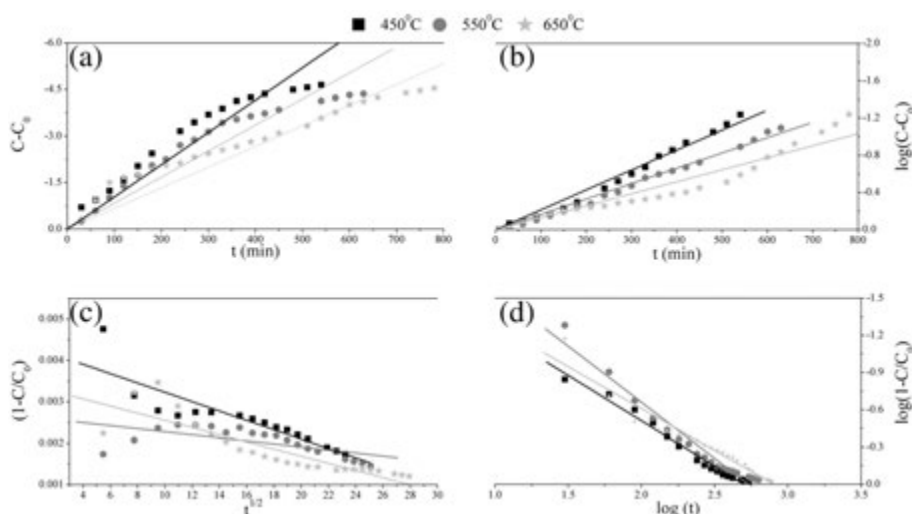


**Figure 12** Photocatalytic degradation kinetics the four models of CR on TiO<sub>2</sub>. (a) Zero-order, (b) first-order, (c) parabolic diffusion, and (d) modified Freundlich models of Congo red on TiO<sub>2</sub> calcined at 450°C, 550°C, and 650°C. The solid lines show linear fitting of the corresponding models.

photocatalytic degradation. The UV-vis reflectance spectra before (curve i) and after illumination with increasing time on synthesized TiO<sub>2</sub> on MB and CR, and reference P25 on MB system are compared in Figures 5, 6, and 7. From this comparison, it is inferred that the complex adsorption bands in the 500- to 750-nm (20,000 to 12,000 cm<sup>-1</sup>) interval, due to adsorption of MB, change rapidly because TiO<sub>2</sub> promotes the catalytic photodegradation (Figure 5, curve b). The photocatalytic degradation of CR has also been investigated (Figure 6). The simple absorption due to CR appears within the range of 400 to 600 nm (approximately 12,000 cm<sup>-1</sup>). The

photocatalytic activity of P25, an excellent TiO<sub>2</sub> photocatalyst, is reported in Figure 7. The disappearance rate within the absorption band of MB on the P25 surface is much faster than that observed in the case of the synthesized TiO<sub>2</sub> calcined at lower temperatures due to lower conversion of hydrogen titanate to TiO<sub>2</sub>. Conversion of TiO<sub>2</sub> is obtained by the subsequent heat treatment of hydrogen titanate at around 300°C to 500°C. A small band was observed at the wavelength of around 600 nm for both cases of TiO<sub>2</sub> (P25) and synthesized TiO<sub>2</sub> samples due to decomposition of the dimers of MB molecules to MB monomers [26]. The results

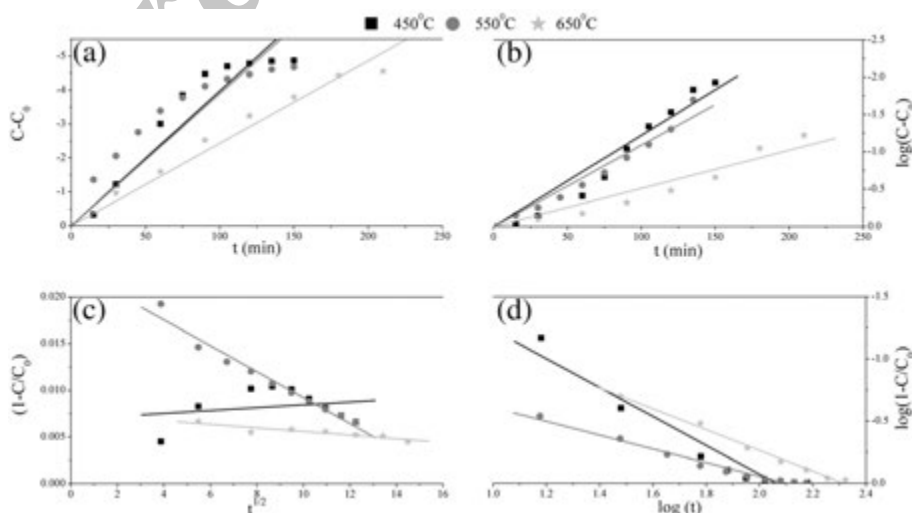


**Figure 13** Photocatalytic degradation kinetics of the four models of MB on P25. (a) Zero-order, (b) first-order, (c) parabolic diffusion, and (d) modified Freundlich models of methylene blue on P25 calcined at 450°C, 550°C, and 650°C. The solid lines show linear fitting of the corresponding models.

**Table 1 Linear correlation coefficients ( $R^2$ ) and photocatalytic degradation rate constant ( $k$ ): MB on synthesized  $\text{TiO}_2$**

Kinetic models	450°C <sup>a</sup>		550°C <sup>a</sup>		650°C <sup>a</sup>	
	$R^2$	$k$	$R^2$	$k$	$R^2$	$k$
Zero-order model	0.89287	-0.01829	0.93596	-0.01548	0.95476	-0.01326
First-order model	0.94183	-0.00555	0.97927	-0.00346	0.93859	-0.00293
Parabolic diffusion model	0.92169	-3.06E <sup>-4</sup>	0.95969	-2.2874E <sup>-4</sup>	0.90039	-1.11E <sup>-4</sup>
Modified Freundlich model	0.95033	0.02225	0.98014	0.018513	0.98018	8.633E <sup>-3</sup>

<sup>a</sup> $\text{TiO}_2$  calcined at 450°C, 550°C, and 650°C.

obtained in this work are in agreement with those of Uddin et al. [13] who found that UV-vis bands of MB at 600 and 660 nm are assigned to the monomeric and aggregated MB (mostly dimeric and trimeric species) adsorbed on the surface. Under exposure to light, the aggregate species disappear first, followed by the monomeric ones. This indicates that the photodegradation destroys not only the conjugate system (including -N = N-) but also the intermediate products partially or totally [27,28]. Between the two dyes, the chemical structure of MB is more susceptible to oxidation by hydroxyl radicals than that of CR. Moreover, it is also possible that MB absorbs less UV light than CR. This would make more photons available to impinge on the catalyst and promote the formation of hydroxyl radicals. However, it must be stated that the degradation between the dyes has been compared on mass basis. On a molar basis, the analysis is much different. The molecular weight of MB and CR are 356 and 697, respectively. This means that the number of moles per parts per million is two times higher for MB, and consequently, the molecular degradation rate of MB is higher than that of CR. As mentioned above, the bands at 660 and 600 nm are assigned to monomeric and aggregated MB, respectively, adsorbed on the  $\text{TiO}_2$  surface, while the CR shows only one absorption band, which explains monomeric layer of CR on the surface. The photocatalytic degradation rate of CR is lower than that of MB due to its weaker adsorption constant ( $K_{\text{ads, CR}} = 2.0 \times 10^{-3}$  L/ $\mu\text{mol}$  and  $K_{\text{ads, MB}} = 6.65 \times 10^{-3}$  L/ $\mu\text{mol}$ ). This fact can be explained by the large steric hindrance arising from the large aromatic ensembles, including one central biphenyl group and two symmetric naphthenic groups [29]. The

photocatalytic degradation kinetics of MB and CR on synthesized  $\text{TiO}_2$  samples and reference P25 is shown in Figures 8, 9, and 10. It is evident from the Figures that the samples calcined at higher temperatures require comparatively more time to complete the photodegradation (Figures 8 and 9) of dyes. At high temperature,  $\text{TiO}_2$  of anatase phase substantially converts to rutile phase, which shows more stability and less photoactivity toward organic strains or dye molecules. It should be noted that the sample calcined at or above 650°C contains a certain amount of rutile  $\text{TiO}_2$ , which lowers the overall photoactivity. The sample calcined at the temperature of 550°C (which results an average particle diameter of 4.0 nm) is efficiently capable of photocatalytic degradation of MB and CR (Figures 8 and 9). It can be concluded that the photocatalytic activity is directly affected by the size of nanoparticles and dye characteristics. The photocatalytic performance of this particular sample is relatively competitive with P25, which is the most effective commercial  $\text{TiO}_2$  photocatalyst.

#### Photocatalytic degradation kinetic models

To explore more into the mechanisms, including successive adsorption and photocatalytic degradation processes at room temperature, four types of kinetic models are applied (zero-order, first-order, parabolic-diffusion, and modified Freundlich model; Figures 11, 12 and 13). A calculation was also made for the corresponding linear correlation coefficients ( $R^2$ ) and photocatalytic degradation rate constant ( $k$ ) (shown in Tables 1, 2, and 3).

The experimental data are analyzed with the selected four types of kinetic models. The experimental data do not fit well to the zero and parabolic diffusion models.

**Table 2 Linear correlation coefficients and photocatalytic degradation rate constant: CR on synthesized  $\text{TiO}_2$**

Kinetic models	450°C <sup>a</sup>		550°C <sup>a</sup>		650°C <sup>a</sup>	
	$R^2$	$k$	$R^2$	$k$	$R^2$	$k$
Zero-order model	0.93855	-0.0104	0.92346	-0.00839	0.96205	-0.00667
First-order model	0.99012	-0.00214	0.99533	-0.00165	0.92984	-0.00129
Parabolic diffusion model	0.76918	-1.13E <sup>-5</sup>	0.40361	-3.66E <sup>-5</sup>	0.76356	-8.63E <sup>-5</sup>
Modified Freundlich model	0.99011	0.01064	0.96032	3.41E-3	0.94501	0.010954

<sup>a</sup> $\text{TiO}_2$  calcined at 450°C, 550°C, and 650°C.



**Table 3 Linear correlation coefficients and photocatalytic degradation rate constant: MB on P25**

Kinetic models	450°C <sup>a</sup>		550°C <sup>a</sup>		650°C <sup>a</sup>	
	R <sup>2</sup>	k	R <sup>2</sup>	k	R <sup>2</sup>	k
Zero-order model	0.9030	-0.03983	0.87677	-0.03901	0.97780	-0.02435
First-order model	0.9672	-0.01222	0.97427	-0.01089	0.94817	-0.00511
Parabolic diffusion model	0.0939	1.5283E <sup>-4</sup>	0.96881	-0.00139	0.83949	-1.931E <sup>-4</sup>
Modified Freundlich model	0.9709	4.0E <sup>-3</sup>	0.97602	0.06904	0.99162	0.0115

<sup>a</sup>P25 calcined at 450°C, 550°C and 650°C.

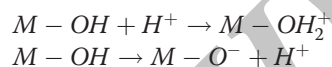
Based on the fitting of kinetic data for the MB and CR adsorption, simultaneous photodegradation on TiO<sub>2</sub> and P25 to the first order and modified Freundlich model, the R<sup>2</sup> values (Tables 1, 2, and 3) are close to unity (0.94 to approximately 0.99) for all cases. From Figures 11, 12, and 13, it can be speculated that the kinetics of adsorption of MB and CR on the as-synthesized titanate nanostructures can be described more accurately by the modified Freundlich kinetic model. This is an indication for the heterogeneous surface binding caused by the monolayer adsorption, and that the molecules follow successive photocatalytic degradation under the UV light illumination. The modified Freundlich model fit the photocatalytic degradation data on synthesized TiO<sub>2</sub> with the linear correlation coefficients of R<sup>2</sup> = approximately 0.98 (Table 1) for MB and R<sup>2</sup> = approximately 0.99 (Table 2) for CR, and the fitted value of k is found to be 0.0086 to 0.0200 units for MB and 0.0030 to 0.0100 units for CR. The modified Freundlich model, in fact, describes heterogeneous diffusion from the flat surfaces via molecular ion exchange. Additionally, the kinetic model prediction suggests similarities in the photocatalytic activity of synthesized TiO<sub>2</sub> and P25. As smaller TiO<sub>2</sub> particles provide more side edges/surfaces and a shorter diffusion path, the bulk dyes can be more readily adsorbed toward the edge/surface in a relatively continuous way even at the beginning of photocatalytic degradation. This result suggests that (1) the system is adsorption-photocatalytic degradation controlled, and (2) the photocatalytic degradation is occurring on the TiO<sub>2</sub> surface.

#### Influence of pH on degradation kinetics

The photocatalytic degradation is studied in the pH range of 2 to 8. From Figure 14, it is evident that the photocatalytic degradation rate increased with the increasing pH, an effect attributed to the variation of the nature and the density of surface charge on the catalyst surface with the change in the pH of the solution.

Adsorption of H<sub>2</sub>O molecules at the surface sites is followed by the dissociation of the -OH groups, leading to coverage with chemically equivalent metal hydroxyl

groups (Ti-OH). For metal hydroxides, the following equilibrium can be considered in aqueous solution:



From the above equations, it is clear that the catalyst surface will be pH sensitive and will assume positive or negative charge depending on the pH of the solution. The zero-point charge (pH<sub>zpc</sub>) of the metal oxide is defined as the pH at which the concentrations of the protonated and deprotonated surface groups are equal. The isoelectric points of TiO<sub>2</sub> may vary over a range of pH depending upon the processing history. This makes the effects of pH on the dissolution of TiO<sub>2</sub> powders in aqueous solutions still unclear. Wang and Ying [30] find the pH<sub>zpc</sub> of TiO<sub>2</sub> to be 6.8. Other authors report that the pH<sub>zpc</sub> of TiO<sub>2</sub> lies between 4 and 6 [31].

At high pH, the catalyst surface is predominantly negatively charged, and a strong interaction occurs between the catalysts surface and the dye cations, resulting in strong adsorption. At low pH, however, both the TiO<sub>2</sub> surface and the dye molecules are positively charged, resulting in weak adsorption. Thus, it is reasonable that with an increase in pH, the adsorption of the dye on the

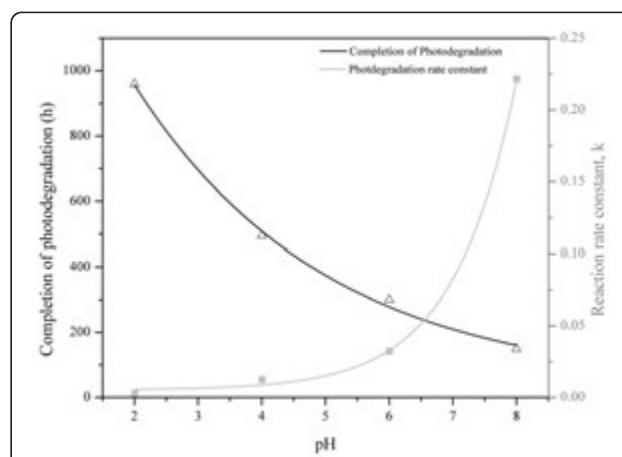


**Figure 14 Photocatalytic degradation of MB on synthesized TiO<sub>2</sub>.** The degradation was conducted to make the relationship between the pH and the rate of photocatalytic degradation.

catalyst surface increases, resulting in higher degradation rate.

## Conclusion

The results reveal that the synthesized TiO<sub>2</sub> nanoparticles can effectively remove MB (98%) and CR (98%) under UV light. Moreover, the photocatalyst can be successfully recovered following exposition under UV light irradiation due to the capacity of the photocatalytic process to mineralize organic compounds by transforming them into carbon dioxide, water, and harmless ions. From this experiment, it is obvious that the higher the calcination temperature of the synthesized TiO<sub>2</sub> nanoparticles, the less the photocatalytic degradation efficiency is, due to appearance of the rutile phase in the TiO<sub>2</sub> nanoparticles, which is unfavorable. It is also found that the modified Freundlich model describes the degradation process very well at higher pH.

## Competing interests

The authors declare that they have no competing interests.

## Authors' contributions

The authors' contributions in this article are the same. All authors read and approved the final manuscript.

## Authors' information

MJU is a Ph.D. degree holder and an associate professor in the Chemical Engineering and Polymer Science Department. MAI is a Ph.D. holder, a professor, and the chair of the said department. MMR is a Ph.D. degree holder and an associate professor in the same department. MSAA is a BS ChE degree holder and an assistant professor in the same department as well. SAH and SH are graduate students of the Chemical Engineering and Polymer Science Department.

## Acknowledgments

This work was funded by a research development fund from Shahjalal University of Science and Technology, Sylhet. The authors express their deep gratitude to Prof. Ulrike Diebold (Tulane University) for providing equipment support for this work and to Prof. M. R. Khan for fruitful discussions.

Received: 4 March 2012 Accepted: 24 July 2012

Published: 30 August 2012

## References

- Herrmann, J.M., Duchamp, C., Karkmaz, M., Hoai, B.T., Lachheb, H., Puzenat, E., Guillard, C.: Environmental green chemistry as defined by photocatalysis. *J. Hazard. Mater.* **145**, 624–629 (2007)
- Diebold, U.: The surface science of titanium dioxide. *Surf. Sci. Rep.* **48**, 55–229 (2003)
- Porkodi, K., Arokiamary, S.D.: Synthesis and spectroscopic characterization of nanostructured anatase titania: a photocatalyst. *Mater. Charact.* **58**, 495–503 (2007)
- Allen, N.S., Edge, M., Verran, J., Stratton, J., Maltby, J., Bygott, C.: Photocatalytic titania based surfaces: environmental benefits. *Polym. Degrad. and Stab.* **93**, 1632–1646 (2008)
- Chen, X., Mao, S.S.: Titanium dioxide nanomaterials: synthesis, properties, modifications, and applications. *Chem. Rev.* **107**, 2891–2959 (2007)
- Cao, F., Oskam, G., Searson, P.C., Stipkala, J.M., Heimer, T.A., Farzad, F., Meyer, G.J.: Electrical and optical properties of porous nanocrystalline TiO<sub>2</sub> films. *J. Phys. Chem.* **99**, 11974–11980 (2007)
- Siegel, R.W.: Cluster-assembled nanophase materials. *Ann. Rev. Mater. Sci.* **21**, 559–578 (1991)
- Yi, K.C., Fendler, J.H.: Between the head groups of Langmuir-Blodgett films. *Langmuir* **6**, 1519–1526 (1990)
- Youn, H.C., Baral, S., Fendler, J.H.: Preparations of nanosized TiO<sub>2</sub> in reverse micro emulsion. *J. Phys. Chem.* **92**, 6320–6327 (1988)
- Fendler, J.H.: Atomic and molecular clusters in membrane mimetic chemistry. *Chem. Rev.* **87**, 877–899 (1987)
- Toba, M., Mizukami, F., Niwa, S., Sano, T., Maeda, K., Annila, A., Komppa, V.: Effect of the type of preparation the 2 properties of titania/silicas. *J. Molec. Catal.* **1**, 277–288 (1994)
- Gao, X., Wachs, E.: Titania-silica as catalysts: molecular structural characteristics and physico-chemical properties. *Catal. Today* **51**, 233–254 (1999)
- Uddin, M.J., Cesano, F., Bonino, F., Bordiga, S., Spoto, G., Scarano, D., Zecchina, A.: Photoactive TiO<sub>2</sub> films on cellulose fibres: synthesis and characterization. *J. Photochem. Photobiol. A-Chem.* **189**, 286–294 (2007)
- Uddin, M.J., Cesano, F., Scarano, D., Bonino, F., Agostini, G., Spoto, G., Bordiga, S., Zecchina, A.: Cotton textile fibres coated by Au/TiO<sub>2</sub> films: synthesis, characterization and self cleaning properties. *J. Photochem. Photobiol. A-Chem.* **199**, 64–72 (2008)
- Liu, Z., Davis, R.J.: Investigation of the structure of microporous Ti-Si mixed oxides by X-ray, UV reflectance, FT-Raman, and FT-IR spectroscopies. *J. Phys. Chem.* **98**, 1253–1261 (1994)
- Uddin, M.J., Cesano, F., Bertarione, S., Bonino, F., Bordiga, S., Scarano, D., Zecchina, A.: Tailoring the activity of Ti-based photocatalysts by playing with surface morphology and silver doping. *J. Photochem. Photobiol. A-Chem.* **196**, 165–173 (2008)
- Wang, L.Y., Sun, Y.P., Xu, B.S.: Comparison study on the size and phase control of nanocrystalline TiO<sub>2</sub> in three Ti-Si oxide structures. *J. Mater. Sci.* **43**, 1979–1986 (2008)
- Jia, Y.X., Han, W., Xiong, G.X., Yang, W.S.: Diatomite as high performance and environmental friendly catalysts for phenol hydroxylation with H<sub>2</sub>O<sub>2</sub>. *J. Colloid Interface Sci.* **323**, 326–331 (2008)
- Zhao, Y., Li, C., Liu, X., Gu, F., Du, H.L., Shi, L.: Zn-doped TiO<sub>2</sub> nanoparticles with high photocatalytic activity synthesized by hydrogen-oxygen diffusion flame. *Appl. Catal. B Environ.* **79**, 208–215 (2008)
- Fox, M.A., Dulay, M.T.: Heterogeneous photocatalysis. *Chem. Rev.* **93**, 341–357 (1993)
- Ollis, D.F., Pelizzetti, E., Serpone, N.: Photocatalyzed destruction of water contaminants. *Environ. Sci. Technol.* **25**, 1522–1529 (1991)
- Gu, Z., Thomas, A.C., Xu, Z.P., Campbell, J.H., Lu, G.Q.: In vitro sustained release of LMWH from MgAl-layered double hydroxide nanohybrids. *Chem. Mater.* **20**, 3715–3722 (2008)
- Kodama, T., Harada, Y., Ueda, M., Shimizu, K., Shuto, K., Komarneni, S.: Selective exchange and fixation of strontium ions with ultrafine Na-4-mica. *Langmuir* **17**, 4881–4886 (2001)
- Li, Z.H.: Sorption kinetics of hexa decyltri methyl ammonium on natural clinop-tilolite. *Langmuir* **15**, 6438–6445 (1999)
- Birks, L.S., Friedman, H.: Particle size determination from X-ray line broadening. *J. Appl. Phys.* **17**, 687–692 (1946)
- Lee, C., Sung, Y.W., Park, J.W.: Multiple equilibria of phenothiazine dyes in aqueous cyclodextrin solutions. *J. Phys. Chem. B* **103**, 893–898 (1999)
- Al-Oaradawi, S., Salman, S.R.: Photocatalytic degradation of methyl orange as a model compound. *J. Photochem. Photobiol. A* **148**, 161–168 (2002)
- Guettai, N., Amar, H.A.: Photocatalytic oxidation of methyl orange in presence of titanium dioxide in aqueous suspension. *Desalination* **185**, 427–437 (2005)
- Lachheb, H., Puzenat, E., Houas, A., Ksibi, M., Elaloui, E., Guillard, C., Herrmann, J.M.: Photocatalytic degradation of various types of dyes (Alizarin S, Crocein orange G, methyl red, methylene blue) in water by UV-irradiated titania. *App. Catal. B Environ.* **39**, 75–90 (2002)
- Wang, C.C., Ying, J.Y.: Sol-gel synthesis and hydrothermal processing of anatase and rutile titania nanocrystals. *Chem. Mater.* **11**, 3113–3120 (1999)
- Chen, Z.C., Ring, T.A., Lemaire, J.: Stabilization of aqueous BaTiO<sub>3</sub> suspension with polyacrylic acid. *J. Am. Ceram. Soc.* **75**, 3201–3208 (1992)

doi:10.1186/2228-5326-2-19

Cite this article as: Uddin et al.: Preparation of nanostructured TiO<sub>2</sub>-based photocatalyst by controlling the calcining temperature and pH. *International Nano Letters* 2012 **2**:19.